Electronic Supplementary Information for

Initial stages of Benzotriazole adsorption on the Cu(111) surface

Federico Grillo, Daniel W. Tee, Stephen M. Francis, Herbert Früchtl, and Neville V. Richardson*

EaStCHEM and School of Chemistry, University of St Andrews, St Andrews, KY16 9ST, United Kingdom

*federico.grillo@st-andrews.ac.uk

SI1. *Calculated vibrational spectra*

Figure SI1 shows the numbering of benzotriazole (BTAH) atoms used throughout the section to describe the molecular vibrations.

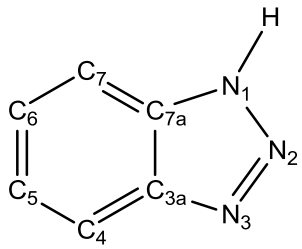

Figure SI1. Numbering scheme of BTAH atoms.

The following vibrational spectra for gas phase species were calculated using the Gaussian 03 software package,[1] with the B3LYP hybrid exchange correlation functional and the 6-311G basis set and no symmetry constraints: BTAH (Figure SI2), BTA^- (Figure SI3), BTA(N_1)-Cu (Figure SI4), BTA(N_2)-Cu (Figure SI5,) and BTA(N_1)-Cu-(N_1)-BTA (Figure SI6, referred as $Cu(BTA)_2$ in the main text). Geometrically optimized structures and corresponding vibrational spectra are reported below; calculated spectra have been corrected according to the formula proposed by Matsuura and Yoshida.[2] Table SI1 reports the experimentally observed modes, a comparison with the calculated ones and their assignments based also upon references.[3-6]

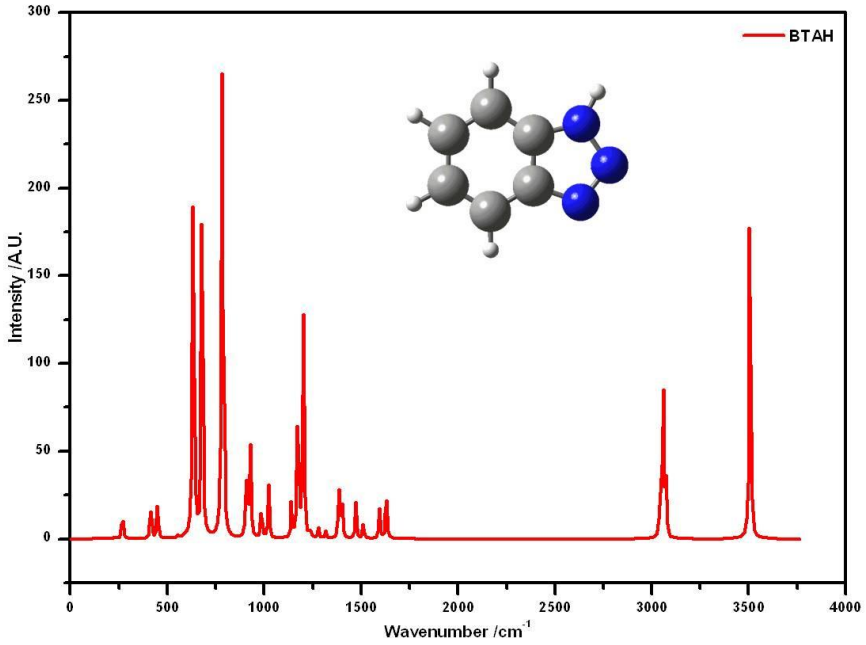

Figure SI2. Geometrically optimized structure of BTAH and calculated infrared spectrum. Atoms in figure; N, blue; C, dark grey; H, light grey.

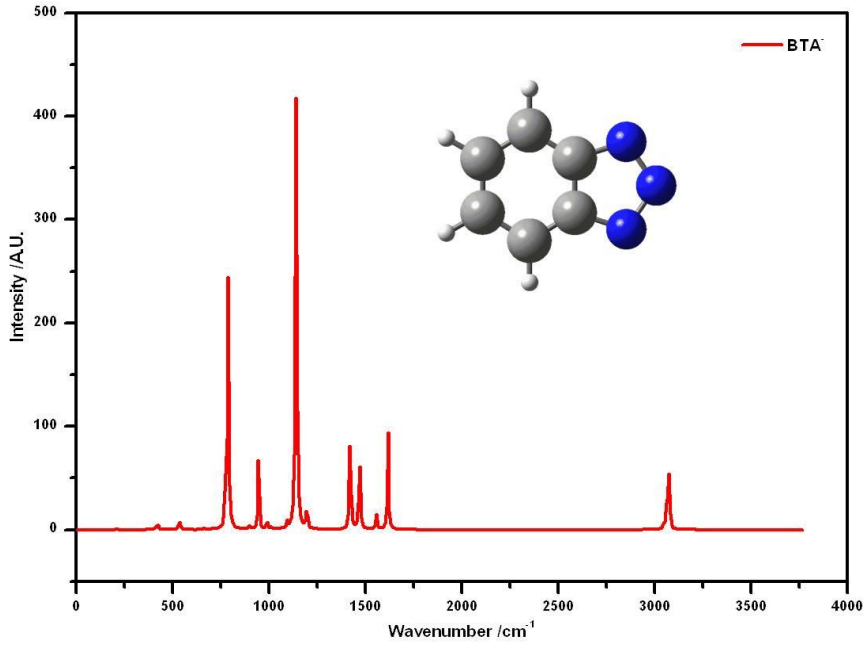

Figure SI3. Geometrically optimized structure of BTA^- and calculated infrared spectrum. Atoms in figure; N, blue; C, dark grey; H, light grey.

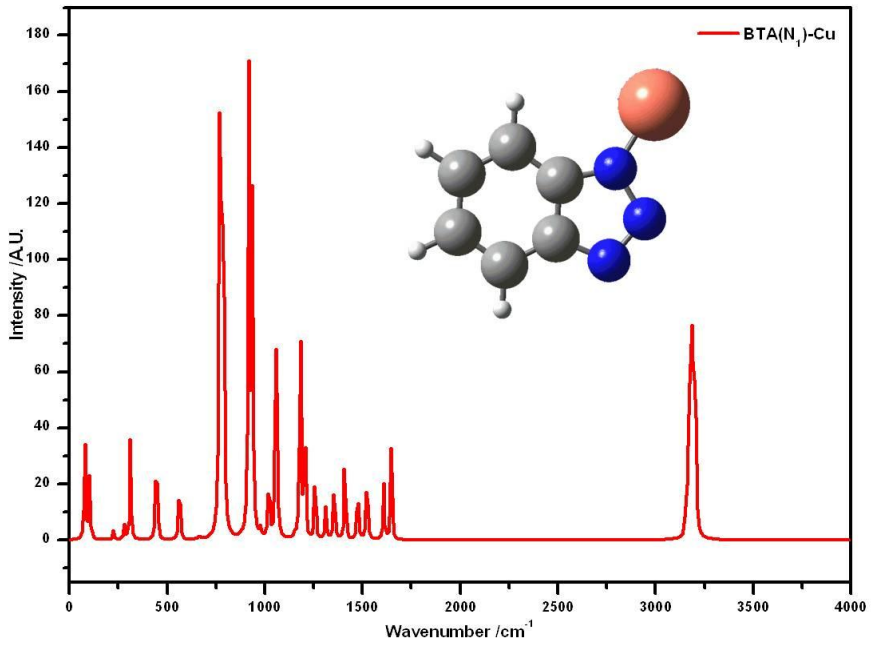

Figure SI4. Geometrically optimized structure of BTA(N_1)-Cu and calculated infrared spectrum. Atoms in figure: Cu, orange; N, blue; C, dark grey; H, light grey.

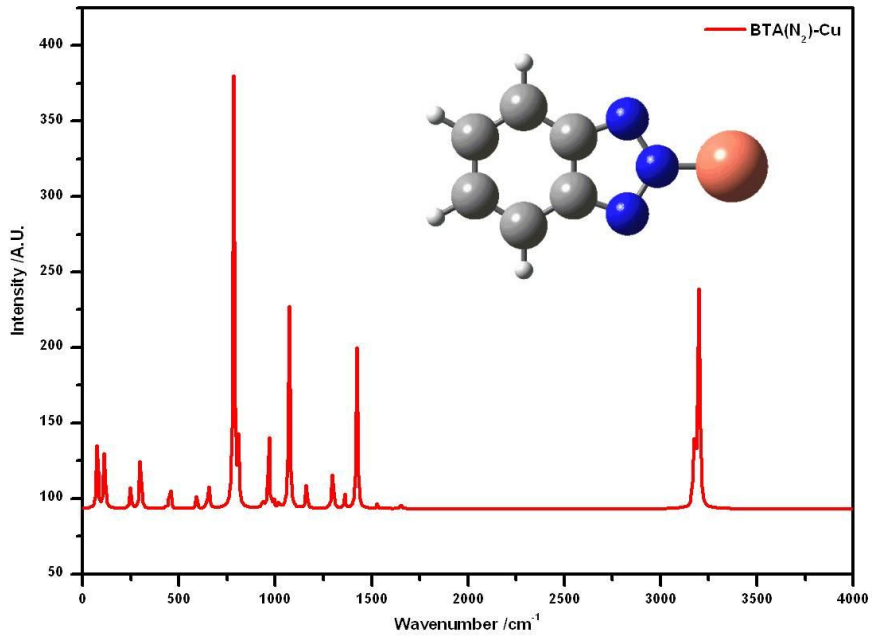

Figure SI5. Geometrically optimized structure of BTA(N_2)-Cu and calculated infrared spectrum. Atoms in figure: Cu, orange; N, blue; C, dark grey; H, light grey.

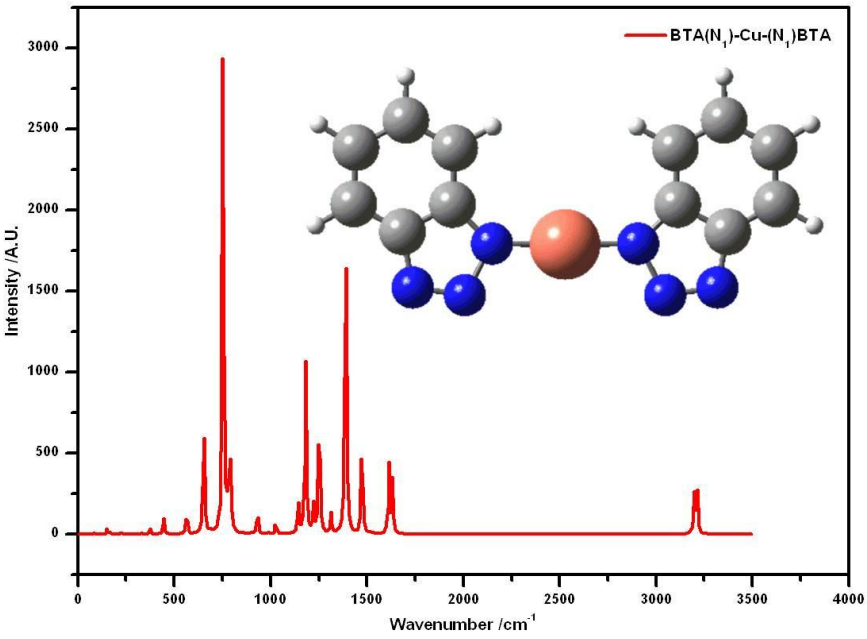

Figure SI6. Geometrically optimized structure of BTA(N_1)-Cu-(N_1)BTA (referred as $Cu(BTA)_2$ in the text) and calculated infrared spectrum. Atoms in figure: Cu, orange; N, blue; C, dark grey; H, light grey.

Table SI1. RAIRS observed peaks (in cm^{-1}) and assignments

Experimental	Calculated*					Assignment (with reference to figure SI1)
	BTAH	BTA^-	N_1-Cu	N_2-Cu	BTA-Cu-BTA	
	3504					ν N-H
3074	3073	3073			3073	ν C-H
3054	3059	3059	3059	3059	3059	ν C-H
		3044	3044	3037		ν C-H
	1632	1617	1621	1624	1602	Aromatic ring in phase ν C_7-C_{7a} + ν C_4-C_5
1573	1594	1556	1579		1586	Aromatic ring in phase ν C_7-C_{7a} + ν C_{3a}-C_4
1511			1494	1502		Aromatic ring in phase ν C_7-C_{7a} + ν C_6-C_7
1486	1471	1471				Aromatic ring out of phase ν C_4-C_5 + ν C_6-C_7
1442			1456		1449	ν C_{3a}-C_{7a}
	1402					δ $C_{7a}N_1$–H
1384	1387	1417	1387	1402	1372	Aromatic ring symmetric breathing
			1333	1341		ν N_3-C_{3a} oop ν N_1-C_{7a}
	1317		1294		1294	ν N_1-C_{7a} + ν N_1-Cu
	1279			1279		ν N_3-C_{3a} + ν C_{3a}-C_4
			1240		1236	ν N_3-C_{3a}
1215	1200	1193	1194		1209	ν N_2-N_3
1168	1170		1170		1170	ν N_2-N_3 + ν N_3-N_{3a}
1122	1139	1138		1147	1132	ν C_6-C_7
1081				1062		ν N_2-N_3 + ν N_1-N_2
	1022		1046			δ N_1-N_2-N_3 scissor
			1007	1007	1015	ν C_5-C_6
979	984		968	984		*w* C-H
	929	944		960		δ N_1-N_2-N_3 scissor

Symbols: ν, stretching; δ, in-plane bending; *w*, wagging; *calculated spectra are corrected according to the formula proposed by Matsuura and Yoshida.[2]

SI2. Additional STM images

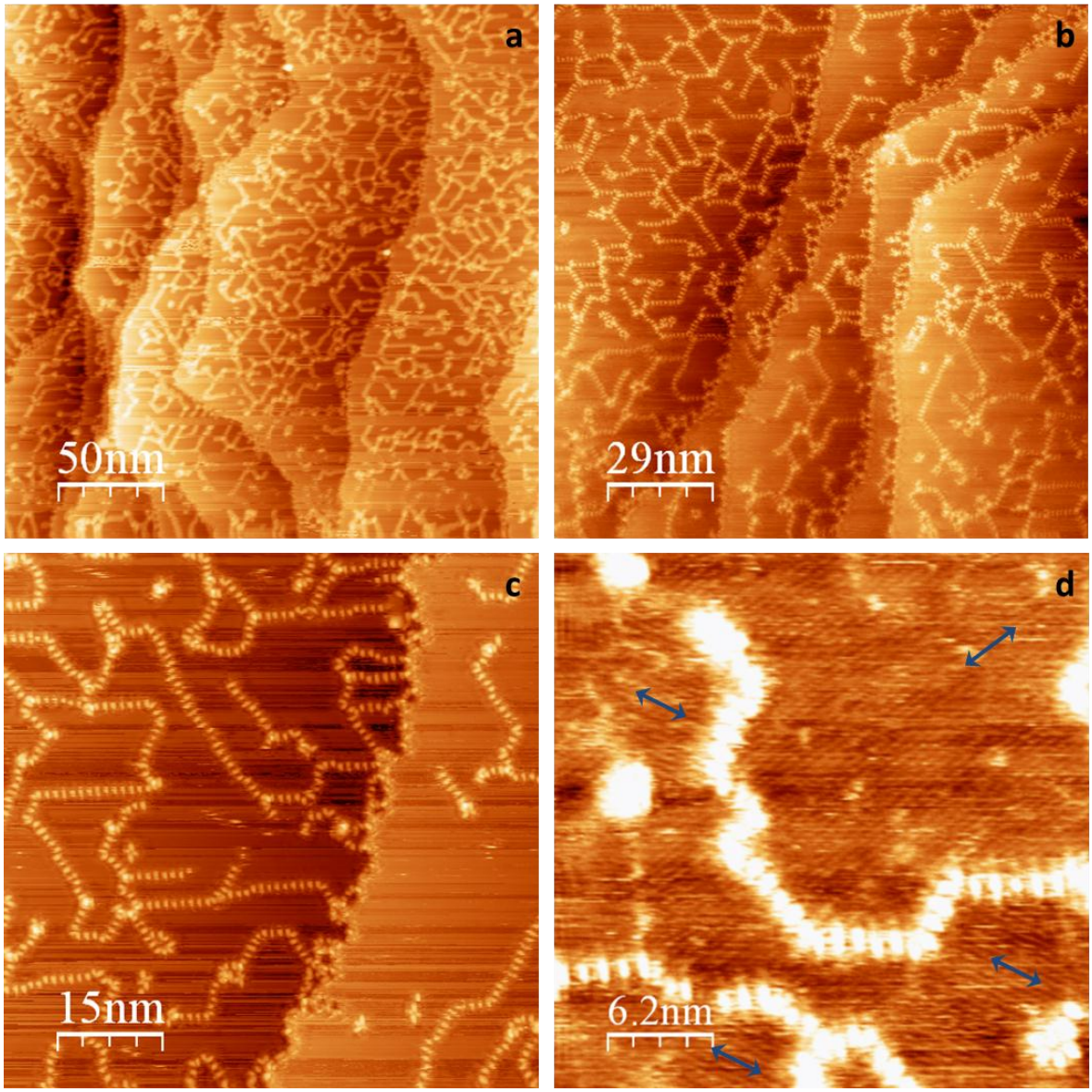

Figure SI7. Molecular chains formed by low coverage BTAH/Cu(111); a) ca. 0.1 ML, 250×250 nm^2, -1.03V, 1.03 nA; b) ca. 0.1 ML, 145×145 nm^2, -1.03V, 0.79 nA; c) ca. 0.05 ML, 75×75 nm^2, -1.07V, 0.91 nA; d) ca. 0.05 ML, 31×31 nm^2, -0.5V, 0.25 nA; enhanced contrast highlighting the superstructure in the areas between the chains attributed to an extended Cu(111)-(2×1) reconstruction; blue arrows indicate the directions of the atomic rows; some horizontal lines, parallel to the fast scanning direction, are due to diffusion of lose species.

SI3. ***Details on the modelling of the 4-unit feature (Figure 3b main text)***

The model in Figure 3b main text was obtained using the SIESTA package employing the PBE functional,[7] a numerical split-valence PAO basis set,[8] with polarization functions (SVP) and Troullier-Martins pseudopotentials,[9] as available from the SIESTA web site. The top gold layer was described using modified strictly localized basis set as reported by García-Gil and co-workers.[10] The free BTA(N_1)-Cu-(N_1)BTA and BTA(N_2)-Cu complexes were initially geometrically optimized using the Gaussian 03 software package[1] with the B3LYP functional and the 6-311g basis set, as previously described. The copper surface was represented by an unreconstructed 10×10×3 slab, whose two bottom layers were kept frozen at the bulk lattice positions; the top layer and the metal-organic complexes were allowed to relax. A vacuum gap corresponding to seven copper layers was used to separate the slabs in the *z* direction. In the initial geometry the $Cu(BTA)_2$ dimers have their longer axis oriented a few degree off the close packed directions and their molecular plains at small angles with the surface normal. The converged geometry is shown in Figure SI8a. For the simulation of the STM image (Figure 3b main and Figure SI8c), LDOS were calculated after geometrical optimization and integrated between the Fermi level (-2.64 eV) and -5 eV (iso value 0.028 e/Bohr^3; rendering WsXM software[11]). Since it was reported that the most stable adsorption geometry for the BTA(N_1)-Cu-(N_1)BTA complex is when the complex longer axis is oriented along <112> directions and the Cu atom on a-top position,[12] a further model, with initial configuration closer to satisfy these conditions, was calculated. The central feature, BTA(N_2)-Cu, was once again adsorbed upright on a 3-fold hollow site. The calculated energy difference for the converged geometries (the second model one is reported in Figure SI8b), shows that the second model would be more stable by ca. 2.83 eV, i.e. ca. 0.4 eV per BTA^-; however, the converged geometry and the calculated STM image for the second model (Figure SI8d, Fermi level -2.63 eV; iso value 0.026 e/Bohr^3; rendering WsXM software[11]) significantly differ

from the experimental findings. Notably, the models proposed do not take into account the observed (2×1) surface reconstruction, which may play an important role in allowing further total energy minimisation of the system. It is worth noting that an extended surface reconstruction was observed for the first time, for this system; none of the theoretical works cited in the introduction section include such feature.

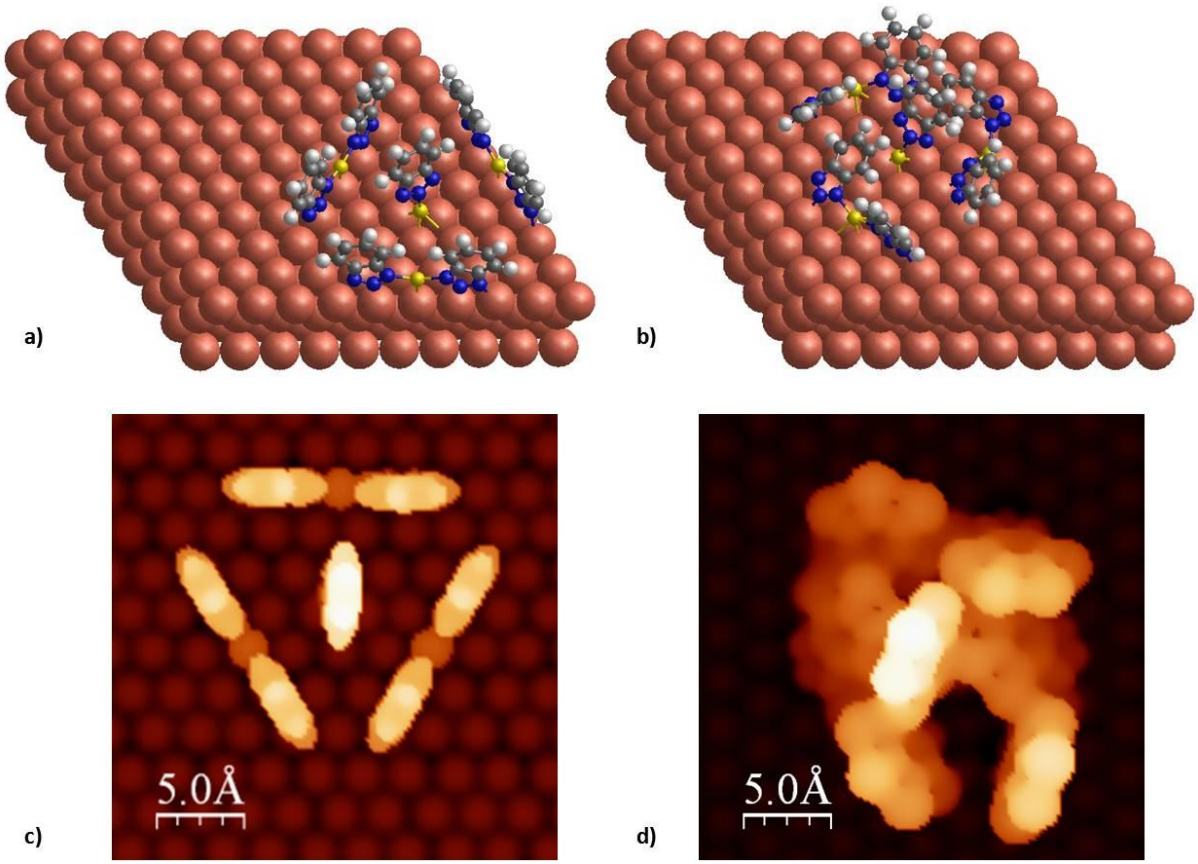

Figure SI8. a) Converged geometry for the 4-units cluster with BTA(N_1)-Cu-(N_1)BTA dimers oriented along <110> directions; b) Converged geometry for the 4-units cluster with BTA(N_1)-Cu-(N_1)BTA dimers initially oriented along <112> directions. Colours key: white, hydrogen; grey, carbon; blue, nitrogen; yellow, copper atoms in the organometallic compound; brown, copper slab; c) calculated STM image for a); d) calculated STM image for b).

SI4. *Statistics on diffusion*

Table SI2 presents the results of the statistical analysis of the diffusing species as reported in figure 4 main text, selecting frames at equal time intervals of five minutes and evaluating the features present on the same 40×40 mn^2 area for each frame. The statistics show that the number of the different adsorbed features stays approximately constant over time. The average first neighbouring distance between the features in the chains is 1.16 ± 0.02 nm, with the standard deviation less than the Cu-Cu atomic spacing in the (111) plane, 0.256 nm. A movie showing diffusion occurring over a period of 111 minutes is available online.

Table SI2: Statistics on diffusion.

Frame number	Time /min	N four units junctions	N loops	N tot	Longest chain length	Most frequent length	First neighbour distance /nm
1	0	23	3	261	18	5	1.171
5	30	17	4	259	15	3	1.153
10	60	17	2	250	20	5	1.120
15	90	17	1	248	14	3	1.151
20	120	16	3	258	16	5	1.193
25	150	18	3	261	15	5	1.201
30	180	18	3	254	17	3	1.156
35	210	17	2	242	18	3	1.162
40	240	15	1	248	17	3	1.178
45	270	17	3	253	17	5	1.164

SI5. Experimental details

Experiments were performed in ultra-high vacuum chambers with a base pressure below 5×10^{-10} mbar and equipped with Low Energy Electron Diffraction (LEED), Scanning Tunnelling Microscopy (VT-STM, Omicron) and RAIRS (Nicolet Nexus 860 FT- IR

spectrometer). The Cu(111) single crystal was cleaned by Ar ion sputtering and annealing cycles until a clean surface, characterized by a sharp (1×1) LEED pattern and large, flat terraces in STM, was observed. STM images were collected in constant current mode using electrochemically etched W tips and were processed using the WSxM software package.[11] BTAH dosing was carried out by electrically heating to ca. 298 K a quartz crucible containing the compound, yielding a deposition rate of ca. 0.5 ML/min, which was reduced to ca. 0.1 ML/min by the introduction of a skimmer between the crucible and the Cu(111) crystal, for the low coverage experiments. RAIR spectra were collected at a resolution of 8 cm^{-1}, 1024 scans; gaseous water and CO_2 contributions were subtracted.

SI6. References

(1) Gaussian 03, Revision E.01; M. J. Frisch, G. W. Trucks, H. B. Schlegel, G. E. Scuseria, M. A. Robb, J. R. Cheeseman, J. A. Montgomery, Jr., T. Vreven, K. N. Kudin, J. C. Burant, J. M. Millam, S. S. Iyengar, J. Tomasi, V. Barone, B. Mennucci, M. Cossi, G. Scalmani, N. Rega, G. A. Petersson, H. Nakatsuji, M. Hada, M. Ehara, K. Toyota, R. Fukuda, J. Hasegawa, M. Ishida, T. Nakajima, Y. Honda, O. Kitao, H. Nakai, M. Klene, X. Li, J. E. Knox, H. P. Hratchian, J. B. Cross, V. Bakken, C. Adamo, J. Jaramillo, R. Gomperts, R. E. Stratmann, O. Yazyev, A. J. Austin, R. Cammi, C. Pomelli, J. W. Ochterski, P. Y. Ayala, K. Morokuma, G. A. Voth, P. Salvador, J. J. Dannenberg, V. G. Zakrzewski, S. Dapprich, A. D. Daniels, M. C. Strain, O. Farkas, D. K. Malick, A. D. Rabuck, K. Raghavachari, J. B. Foresman, J. V. Ortiz, Q. Cui, A. G. Baboul, S. Clifford, J. Cioslowski, B. B. Stefanov, G. Liu, A. Liashenko, P. Piskorz, I. Komaromi, R. L. Martin, D. J. Fox, T. Keith, M. A. Al-

Laham, C. Y. Peng, A. Nanayakkara, M. Challacombe, P. M. W. Gill, B. Johnson, W. Chen, M. W. Wong, C. Gonzalez, J. A. Pople, Gaussian, Inc., Wallingford CT, 2004.

(2) H. Matsuura, H. Yoshida, *Handbook of Vibrational Spectroscopy*, vol. 3, S4203, Wiley (2001).

(3) I. Popopva, J. T. Yates Jr., *Langmuir*, 1997, **13**, 6169.

(4) C. Törnkvist, J. Bergman, B. Liedberg, *J. Phys. Chem.*, 1991, **95(8)**, 3119.

(5) N. R. Honesty, A. A. Gewirth, *J. Raman Spectroscopy*, 2012, **43**, 46.

(6) K. Salorinne, X. Chen, R. W. Troff, M. Nissinen, H. Häkkinen, *Nanoscale*, 2012, **4**, 4095.

(7) J. P. Perdew, K. Burke, M. Ernzerhof, *Phys. Rev. Lett.,* 1996, **77**, 3865.

(8) O. F. Sankey, D. J. Niklewski, *Phys. Rev. B,* 1989, **40**, 3979.

(9) N. Troullier, J. L. Martins, *Phys. Rev. B,* 1991, **43**, 1993.

(10) S. García-Gil, A. García, N. Lorente, P. Ordejón, *Phys. Rev. B,* 2009, **79**, 075441.

(11) I. Horcas, R. Fernández, J. M. Gómez-Rodríguez, J. Colchero, J. Gómez-Herrero, A. M. Baro, *Rev. Sci. Instrum.*, 2007, **78**, 013705.

(12) X. Chen, H. Häkkinen, *J. Phys. Chem. C*, 2012, **116**, 22346.